

CP Violation in $\gamma\gamma \rightarrow t\bar{t}$ within the Minimal Supersymmetric Standard Model

Zhou Mian-Lai^b, Ma Wen-Gan^{a,b,c}, Han Liang^b,
Jiang Yi^b and Zhou Hong^b

^aCCAST (World Laboratory), P.O.Box 8730, Beijing 100080, China

^bModern Physics Department, University of Science and
Technology of China, Anhui 230027, China

^cInstitute of Theoretical Physics, Academia Sinica, P.O.Box 2735, Beijing 100080, China.

Abstract

The complete analysis of the CP violation in the process $\gamma\gamma \rightarrow t\bar{t}$ in frame of the Minimal Supersymmetric Model(MSSM) is presented. The CP-odd observables for describing the CP violating effects in polarized and unpolarized photon collisions, are calculated. We investigate the possible CP violation sources induced by the complex soft breaking parameters and study the CP violating effects contributed by gluino, neutralino and chargino sectors appearing in the loop diagrams. We find that it is possible to observe the CP violating effects in top quark pair production via polarized and unpolarized photon fusions by using optimal observables and favorable parameters.

PACS: 11.30.Er, 12.60.Fr, 14.65.Ha, 13.88.+e

I. Introduction

Since the first discovery of CP violation in the kaon system over thirty years ago [1], CP violating phenomena have been investigated and discussed extensively by a lot of physicists. Various models have been proposed to explain the CP violation observed in $K^0 - \bar{K}^0$ mixing [2]. Although the Cabibbo-Kobayashi-Maskawa(CKM) [3] mechanism in the Standard Model(SM) can explain all the currently available experimental data of CP violation, there is still some room for the extended models of the SM, which can explain the CP violation phenomena equivalently well. Moreover, in cosmology theory there is a so-called baryon genesis problem of the universe [4], and the strength of CP violation due to the CKM mechanism is not strong enough. It indicates some new source(s) of CP violation is required. Therefore, the origin of CP violation still remains a puzzle. The Standard Model accommodated with the complex phase in CKM matrix gives the CP violating interactions, but its predicted CP violating effects outside the K-, D-, and B-meson systems are greatly suppressed at high energy scale and hence unobservably small [5]. That is to say, the experimental and theoretical discovery of strong CP violation at large energy scale would probably reveal new physics beyond the Standard Model, in which the CP violating effects might be considerably enhanced, especially in the processes involving heavy quarks. Thus, we shall concentrate on the observable effects of CP violation induced by non-standard model interactions.

Recently the evidence for the existence of the top quark has been found experimentally by the CDF Collaboration with the top quark mass determined being in the range of 170-200 GeV[6], which coincides with the indirect determination from the precise data of electroweak experiments. Because of the large mass of the top quark, it is believed possible to probe the CP violation from the reactions involving top quarks. Since then a lot of research has been carried on the CP violation in top quark pair production. A. Bartl et.al. presented a complete analysis of electric and weak dipole moment form factors of top quark with complex supersymmetric parameters in [7]. References [8] [9] [10] and [11] discussed the CP violation in the process $e^+e^- \rightarrow t\bar{t}$, while the CP asymmetry in the top quark pair production at hadron colliders was investigated in Ref.[12] [13] [14] and [15]. It is known that the process $\gamma\gamma \rightarrow t\bar{t}$ has more advantages in the probing of CP violation because the production of top quark pairs via photon-photon collision is much cleaner than at pp or $p\bar{p}$ colliders, and its production rate from back-scattering photons is much larger than that from the direct $e^+e^- \rightarrow t\bar{t}$ production. At the Next Linear Col-

lider (NLC), a large number of top quark pairs are produced with large statistical events [16]. On this aspect, Anlauf et.al. discussed CP violation in a Higgs mediated $\gamma\gamma \rightarrow t\bar{t}$ process and studied the triple-product correlations as well as other asymmetric parameters [17]. Poulose et.al. also analyzed the electric dipole moment of the top quark which leads to the CP violating asymmetries[11]. And Han Liang et.al. investigated the QCD corrections to the cross section and the CP violating effects of $\gamma\gamma \rightarrow t\bar{t}$ with both polarized and unpolarized initial particles [18].

In this paper we study CP violation in the process $\gamma\gamma \rightarrow t\bar{t}$ in the framework of the Minimal Supersymmetric Standard Model(MSSM) [19]. It is the simplest case of the SUSY model and the currently most favorite extension of the Standard Model. In this model some strong CP violating interactions may be introduced, which would enhance the CP violation effects greatly. As we know, in the SM, the mixing of top quark with other generation is very small because of the unitary of the CKM matrix, the corresponding CP violation in this process would be negligibly small. However, in the MSSM, new source(s) of CP violation can be induced by additional complex couplings within one generation [20]. This feature provides us with the possibilities to investigate the strong CP violating phenomena in the process $\gamma\gamma \rightarrow t\bar{t}$ within the MSSM.

We organized the paper as follows. In Section II, we introduce two CP-odd observables respectively for polarized and unpolarized photon collisions, and analyze the CP asymmetries caused by the complex interactions in the frame of the MSSM at one-loop level. Then in Section III, the numerical calculation and discussion are presented. Finally, a short summary is given. In Appendix we listed the explicit forms of the transformation matrices U , V , and N .

II. CP-odd Observables

In this paper, we denote the process as:

$$\gamma(p_3, \lambda_1)\gamma(p_4, \lambda_2) \rightarrow t(p_1, s_1)\bar{t}(p_2, s_2), \quad (2.1)$$

where p_1 , p_2 , p_3 and p_4 represent the four-momenta of the outgoing top quark pair and incoming photons respectively, whereas s_1 , s_2 , λ_1 and λ_2 denote the spin four-momenta of top quark pair and the polarizations of incoming photons, respectively.

The Feynman diagrams for the process (2.1) at the tree-level are shown in Fig.1(a) and the one-loop diagrams which contribute to CP violating effect in the frame of the MSSM are plotted in Fig.1(b)-(j). The relevant Feynman rules can be

found in Ref. [19]. Including all the diagrams appearing in Fig.1, the renormalized amplitude for $t\bar{t}$ pair production in $\gamma\gamma$ collision is shown as

$$\begin{aligned}
M_{ren}(\lambda_1, \lambda_2, s_1, s_2) &= M_{tree}(\lambda_1, \lambda_2, s_1, s_2) + M_{one-loop}^{CP}(\lambda_1, \lambda_2, s_1, s_2) \\
&= M_{tree}(\lambda_1, \lambda_2, s_1, s_2) + M_{self-energy}^{CP}(\lambda_1, \lambda_2, s_1, s_2) + M_{vertex}^{CP}(\lambda_1, \lambda_2, s_1, s_2) \\
&\quad + M_{box}^{CP}(\lambda_1, \lambda_2, s_1, s_2) + M_{quartic}^{CP}(\lambda_1, \lambda_2, s_1, s_2) \\
&= \epsilon_\mu(p_3, \lambda_1)\epsilon_\nu(p_4, \lambda_2)\bar{u}(p_1, s_1)[f_1\gamma^\mu\gamma^\nu + f_2\gamma^\nu\gamma^\mu + f_3p_1^\nu\gamma^\mu + f_4p_2^\nu\gamma^\mu \\
&\quad + f_5p_1^\mu\gamma^\nu + f_6p_2^\mu\gamma^\nu + f_7p_1^\mu p_1^\nu + f_8p_1^\mu p_2^\nu + f_9p_2^\mu p_1^\nu + f_{10}p_2^\mu p_2^\nu \\
&\quad + f_{11}p_3^\mu\gamma^\nu + f_{12}p_3^\nu\gamma^\mu + f_{13}p_3^\mu p_1^\nu + f_{14}p_3^\nu p_2^\mu + f_{15}p_3^\mu p_1^\mu \\
&\quad + f_{16}p_3^\mu p_2^\nu + f_{17}p_3^\mu p_1^\nu + f_{18}p_3^\mu p_2^\nu + f_{19}p_3^\mu p_2^\mu + f_{20}p_3^\mu p_2^\nu \\
&\quad + f_{21}\gamma_5\gamma^\mu\gamma^\nu + f_{22}\gamma_5\gamma^\nu\gamma^\mu + f_{23}\gamma_5p_1^\nu\gamma^\mu + f_{24}\gamma_5p_2^\nu\gamma^\mu + f_{25}\gamma_5p_1^\mu\gamma^\nu \\
&\quad + f_{26}\gamma_5p_2^\mu\gamma^\nu + f_{27}\gamma_5p_1^\mu p_1^\nu + f_{28}\gamma_5p_1^\mu p_2^\nu + f_{29}\gamma_5p_2^\mu p_1^\nu + f_{30}\gamma_5p_2^\mu p_2^\nu \\
&\quad + f_{31}\gamma_5p_3^\mu\gamma^\nu + f_{32}\gamma_5p_3^\nu\gamma^\mu + f_{33}\gamma_5p_3^\mu p_1^\nu + f_{34}\gamma_5p_3^\nu p_2^\mu \\
&\quad + f_{35}\gamma_5p_3^\mu p_1^\nu + f_{36}\gamma_5p_3^\mu p_2^\nu + f_{37}\gamma_5p_3^\mu p_1^\mu + f_{38}\gamma_5p_3^\mu p_2^\mu \\
&\quad + f_{39}\gamma_5p_3^\mu p_2^\nu + f_{40}\gamma_5p_3^\mu p_2^\nu]v(p_2, s_2). \tag{2.2}
\end{aligned}$$

Our calculation shows that the form factor coefficients $f_i(i = 1, 2, \dots, 20)$ turn out to have no effect on CP violation, but they contribute to the total cross section at one-loop order. On the other hand, the other 20 form factor coefficients affect CP-odd observables, but do not appear in the total cross section of the process when the polarizations of initial states and spins of final states are summed up. It should be noticed that all the terms in Eq.(2.2) involving $f_i(i = 21, 22, \dots, 40)$ contain γ_5 , while the others which involve $f_i(i = 1, 2, \dots, 20)$ do not.

Concerning the CP violation in process (2.1), three types of couplings may have contributions to CP asymmetry: gluino in the vertex $t\tilde{t}g$, chargino in the vertex $t\tilde{b}\tilde{\chi}^+$ and neutralino in the vertex $t\tilde{t}\tilde{\chi}^0$. Although generally speaking the contribution from gluino diagram is much larger than that from the chargino and neutralino sectors because of the strong coupling which is proportional to $\alpha_s = \frac{g_s^2}{4\pi}$, the following numerical calculation shows that there are still some occasions when the contributions from the latter two sectors are enhanced to be comparable to the gluino contribution. Therefore, we shall consider all the CP violating sources from the mechanism of the MSSM in our calculation.

According to the analysis in the MSSM theory, the CP violation in the interactions involving top quark may be attributed to the imaginary parts of several soft

breaking parameters. The complex phases of supersymmetric soft breaking trilinear couplings $\arg(A_t)$ and $\arg(A_b)$, enter in the scalar quark mixing when the current eigenstates are transformed to the mass eigenstates:

$$\begin{aligned}\tilde{q}_L &= (\tilde{q}_1 \cos \theta_q + \tilde{q}_2 \sin \theta_q) e^{-i\phi_q} \\ \tilde{q}_R &= (-\tilde{q}_1 \sin \theta_q + \tilde{q}_2 \cos \theta_q) e^{i\phi_q}.\end{aligned}\quad (2.3)$$

The complex phases of the higgsino mass parameter μ and $SU(3)$, $U(1)$ gaugino mass parameters (i.e., ϕ_μ , $\phi_{SU(3)}$ and $\phi_{U(1)}$) enter in the couplings of top quark with the gluino, chargino and neutralino through the transformation matrices U , V , and N (see Appendix). The complex phases of other soft breaking parameters, such as $\phi_{SU(2)}$, can be set to be zero without loss of generality, since they can be rotated away through suitable redefinition of the fields.

We firstly consider the process via the collisions of polarized photon beams with photon polarizations denoted as λ_1 and λ_2 , not measuring the spins of the final top quark pair. For the photon's polarization vectors, we use the following formula:

$$\epsilon^\mu(p, \lambda)\epsilon^{\nu*}(p, \lambda') = \frac{\delta_{\lambda, \lambda'}}{2} \left(-g^{\mu\nu} + \frac{p^\mu k^\nu + p^\nu k^\mu}{(p \cdot k)} + i\lambda\epsilon^{\sigma\mu\rho\nu} \frac{p_\sigma k_\rho}{(p \cdot k)} \right), \quad (2.4)$$

where k is an arbitrary light-like Lorentz vector. In order to describe the CP violating effects in the process with the polarized initial states, we introduce a CP-odd observable defined as

$$\xi_{CP} = \frac{\sigma_{++} - \sigma_{--}}{\sigma_{++} + \sigma_{--}}, \quad (2.5)$$

where the lower indexes appearing in the right hand of the equation denote the helicities of the incoming photons (i.e., the λ_1 and λ_2), $\sigma_{\pm\pm}$ represent the cross section of the process (2.1) with initial photons being polarized and the spins of final tops being summed up. The cross section for this process including the one-loop order supersymmetric corrections of CP violation is expressed as

$$\begin{aligned}\sigma &= \langle |M_{total}|^2 \rangle = \langle |M_{tree} + M_{one-loop}^{CP}|^2 \rangle \\ &\simeq \langle |M_{tree}|^2 \rangle + 2 \langle \text{Re}(M_{tree}^\dagger M_{one-loop}^{CP}) \rangle.\end{aligned}\quad (2.6)$$

Here the notation $\langle \rangle$ means taking the integration over the phase space. It is known that at the tree level the cross sections with photon helicities $++$ and $--$

have the same value, and the interference term in Eq.(2.6) is much smaller than the tree level term. Therefore, Eq.(2.5) can be rewritten as following:

$$\xi_{CP} \simeq \text{Re} \left(\frac{<(M_{tree}^\dagger M_{one-loop}^{CP})_{++}> - <(M_{tree}^\dagger M_{one-loop}^{CP})_{--}>}{<|M_{tree}|_{++}^2>} \right). \quad (2.7)$$

Similarly, the lower indexes $\pm\pm$ appearing above represent the initial photon helicities in the one-loop diagrams which contribute to CP violation. Eq.(2.7) is just the practical expression used in our calculation for the observable ξ_{CP} .

Secondly, we consider the CP violating effects in the process (2.1) with unpolarized photon beams. We assume that the final states are polarized, and denote the spin vectors of top and anti-top quarks as s_1 and s_2 , respectively. These spin four-vectors should satisfy:

$$s_i \cdot s_i = -1, \quad s_i \cdot p_i = 0, \quad (i = 1, 2) \quad (2.8)$$

which are introduced by Bjorken and Drell [22] for the massive fermion case. In the rest frame of top quark, the spatial part of the spin vector defined above points in the direction of top quark's spin. The wave functions with spin vectors should satisfy the Bjorken-Drell expressions:

$$\begin{aligned} u(p, s)\bar{u}(p, s) &= \frac{1}{2}(\not{p} + m)(1 + \gamma_5 \not{s}), \\ v(p, s)\bar{v}(p, s) &= \frac{1}{2}(\not{p} - m)(1 + \gamma_5 \not{s}). \end{aligned} \quad (2.9)$$

The connection of this kind of definition with the commonly used spinor helicity basis method is presented in Ref.[23]. The CP-odd observable η_{CP} for the unpolarized photon collisions is defined as

$$\eta_{CP} = \hat{p}_1 \cdot (\vec{s}_1 \times \vec{s}_2). \quad (2.10.a)$$

The expectation value of η_{CP} should be

$$\bar{\eta}_{CP} = \frac{<\sum_{s_1, s_2} [d\sigma(s_1, s_2)(\hat{p}_1 \cdot (\vec{s}_1 \times \vec{s}_2))]>}{\sigma_{total}}, \quad (2.10.b)$$

where \hat{p}_1 is the unit vector of the spatial part of p_1 , \vec{s}_1 and \vec{s}_2 are the spatial parts of the spin vectors s_1 and s_2 , respectively. The summation in the right hand of

the Eq.(2.10.b) should be performed over all the possible spins of top quark pair. Note that the component of top(anti-top) quark's spin vector along its momentum has no contribution to the triple product observable η_{CP} , thus we only consider the top(anti-top) quark spin with its spatial component in the direction perpendicular to vector \vec{p}_1 . In order to satisfy Eq.(2.8), we choose the time parts of s_1 and s_2 to be zero and \vec{s}_1 and \vec{s}_2 to be unit vectors lying on the plane perpendicular to $\vec{p}_1(\vec{p}_2)$. If we define $\theta_1(\theta_2)$ as the angle between $\vec{s}_1(\vec{s}_2)$ and the reaction plane, our calculation shows that the interference term appearing in Eq.(2.6) can be expressed as the function of $\cos \theta_1$, $\cos \theta_2$, $\sin \theta_1$ and $\sin \theta_2$:

$$\begin{aligned} 2Re(M_{tree}^\dagger(s_1, s_2)M_{one-loop}^{CP}(s_1, s_2)) = & C_0 + C_1 \cos \theta_1 + C_2 \cos \theta_2 + \\ & C_3 \sin \theta_1 + C_4 \sin \theta_2 + \\ & C_5 \cos \theta_1 \cos \theta_2 + \\ & C_6 \sin \theta_1 \sin \theta_2 + \\ & C_7 \cos \theta_1 \sin \theta_2 + \\ & C_8 \sin \theta_1 \cos \theta_2, \end{aligned} \quad (2.11)$$

To evaluate the observable $\bar{\eta}_{CP}$, here we introduce Cartesian coordinate frame(x, y, z) in the CMS of this reaction. In this frame, \hat{z} is a unit vector along the outgoing direction of top quark, whereas \hat{x} is defined in the production plane of top quark pair, and both \hat{x} and \hat{y} are located in the plane perpendicular to the outgoing direction of top quark. Then all the orthogonal combinations of the top and anti-top's spins, which have non-zero contributions to CP-odd observable $\bar{\eta}_{CP}$, are listed below:

- (1) $s_1 = (0, +\hat{x}) = (0, +1, 0, 0)$, $s_2 = (0, +\hat{y}) = (0, 0, +1, 0)$;
- (2) $s_1 = (0, +\hat{x}) = (0, +1, 0, 0)$, $s_2 = (0, -\hat{y}) = (0, 0, -1, 0)$;
- (3) $s_1 = (0, -\hat{x}) = (0, -1, 0, 0)$, $s_2 = (0, +\hat{y}) = (0, 0, +1, 0)$;
- (4) $s_1 = (0, -\hat{x}) = (0, -1, 0, 0)$, $s_2 = (0, -\hat{y}) = (0, 0, -1, 0)$;
- (5) $s_1 = (0, +\hat{y}) = (0, 0, +1, 0)$, $s_2 = (0, +\hat{x}) = (0, +1, 0, 0)$;
- (6) $s_1 = (0, +\hat{y}) = (0, 0, +1, 0)$, $s_2 = (0, -\hat{x}) = (0, -1, 0, 0)$;
- (7) $s_1 = (0, -\hat{y}) = (0, 0, -1, 0)$, $s_2 = (0, +\hat{x}) = (0, +1, 0, 0)$;
- (8) $s_1 = (0, -\hat{y}) = (0, 0, -1, 0)$, $s_2 = (0, -\hat{x}) = (0, -1, 0, 0)$.

Because that the contribution from tree-level cross section to Eq.(2.10.b) turns out to be zero, only the interference term between the tree level amplitude and the CP violating one-loop amplitudes should be evaluated. By using Eq.(2.11) and Eq.(2.12), the observable $\bar{\eta}_{CP}$ can be worked out as

$$\bar{\eta}_{CP} = \frac{\langle \sum_{s_1, s_2} [2\text{Re}(M_{\text{tree}}^\dagger M_{\text{one-loop}}^{CP})(\hat{p}_1 \cdot (\vec{s}_1 \times \vec{s}_2))] \rangle}{\sigma_{\text{total}}} = \frac{4 \langle C_8 - C_7 \rangle}{\sigma_{\text{total}}}. \quad (2.13)$$

In our calculation, the dimensional reduction method and the on-mass-shell(OMS) renormalization scheme are adopted to eliminate the ultraviolet divergences appearing at one-loop order[21]. The detailed steps and formula of renormalization can be referred to Ref.[18]. The explicit evaluation demonstrate that the vertex and self-energy diagrams shown in Fig.1 have no contribution to ξ_{CP} , but contribute to $\bar{\eta}_{CP}$, when the CP-violating phases are not all zero.

III. Numerical Calculations and Discussions

The two CP-odd observables defined above are strongly related with the CP violating parameters involved in the Yukawa couplings with top quark, i.e., $V_{t\tilde{t}\tilde{g}}$, $V_{t\tilde{t}\tilde{\chi}^0}$, and $V_{t\tilde{t}\tilde{\chi}^0}$. The corresponding Lagrangians of the interactions can be written as

$$\begin{aligned} \mathcal{L}_{\bar{t}_\alpha \tilde{t}_\beta \tilde{g}_\gamma} &= -\sqrt{2}g_s T_{\alpha\beta}^\gamma \bar{t}_\alpha (P_R \tilde{t}_L^\beta - P_L \tilde{t}_R^\beta) \tilde{g}_\gamma e^{i\phi_{SU(3)}} + h.c. \\ \mathcal{L}_{\bar{t} \tilde{t} \tilde{\chi}_i^0} &= -\sqrt{2}g \bar{t} \tilde{t}_L \tilde{\chi}_i^0 \left\{ \frac{m_t}{2m_W \sin \beta} P_L N_{i4}^* + \left(\frac{1}{6} \tan \theta_W N_{i1} + \frac{1}{2} N_{i2} \right) P_R \right\} \\ &\quad + \sqrt{2}g \bar{t} \tilde{t}_R \tilde{\chi}_i^0 \left\{ -\frac{m_t}{2m_W \sin \beta} P_R N_{i4} + \frac{2}{3} \tan \theta_W P_L N_{i1}^* \right\} + h.c. \\ \mathcal{L}_{\bar{t} \tilde{b} \tilde{\chi}_i^+} &= -g \bar{t} \tilde{b}_L P_R U_{i1} \tilde{\chi}_i^+ + \frac{gm_b}{\sqrt{2}m_W \cos \beta} \bar{t} \tilde{b}_R P_R U_{i2} \tilde{\chi}_i^+ \\ &\quad + \frac{gm_t}{\sqrt{2}m_W \sin \beta} \bar{t} \tilde{b}_L P_L V_{i2}^* \tilde{\chi}_i^+ + h.c., \end{aligned} \quad (3.1)$$

where $T_{\alpha\beta}^\gamma$ are the SU(3) generators, α, β, γ are the color indices, g_s and g are the strong and weak coupling constant, and $P_{R,L} = (1 \pm \gamma_5)/2$. It can be seen that the squark mixing angles $\theta_{\tilde{q}}$ and phases $\phi_{\tilde{q}}$ ($\tilde{q} = \tilde{t}, \tilde{b}$) are involved in the couplings when we express the Lagrangian with the mass eigenstates \tilde{q}_1, \tilde{q}_2 instead of the

weak eigenstates \tilde{q}_L, \tilde{q}_R . Because normally the CP effects from the gluino sector is much more important than from the chargino and neutralino sectors, the most considerable contribution of the squark mixing phases to CP violation is the effect of the phase angle $\phi_{\tilde{t}}$ on the vertex of top-stop-gluino.

The CP violating effects may be induced by the complex phases of $SU(3)$, $U(1)$ mass parameters and Higgs mass parameter μ , wherein $\phi_{SU(3)}$ only emerges in the gluino sector through the Majorana mass term [24], $\phi_{U(1)}$ is only involved in the neutralino sector through the diagonalizing matrix N , and ϕ_μ impresses both neutralino and chargino sectors through matrices U , V and N . It should be noticed that these phases take parts in the CP violation not only through the chargino and neutralino mass transformation matrices, but also through their mass spectra. The chargino and neutralino masses may vary by about one half of their original values when these complex phases are varied.

Although there are some constraints on the supersymmetric parameters in the theory, such as grand unification(GUT), in the following analysis we do not put any extra limitations on them for the general discussion. In the numerical calculation, we assume the following corresponding input parameters by default, in case that no special declaration has been presented on them:

$$\begin{aligned}
\sqrt{\hat{s}} &= 600 \text{ GeV}, \quad \tan \beta = 2, \quad m_{\tilde{g}} = 150 \text{ GeV}, \\
m_{\tilde{t}_1} &= 150 \text{ GeV}, \quad m_{\tilde{t}_2} = 400 \text{ GeV}, \quad m_{\tilde{b}_1} = 270 \text{ GeV}, \quad m_{\tilde{b}_2} = 280 \text{ GeV}, \\
\theta_{\tilde{t}} &= \theta_{\tilde{b}} = \pi/6, \quad \phi_{\tilde{t}} = \phi_{\tilde{b}} = \pi/5, \\
|M_{U(1)}| &= 320 \text{ GeV}, \quad M_{SU(2)} = 250 \text{ GeV}, \quad |\mu| = 220 \text{ GeV}, \\
\phi_{U(1)} &= \pi/4, \quad \phi_{SU(3)} = 0, \quad \phi_\mu = 4\pi/3,
\end{aligned} \tag{3.2}$$

Our calculation shows that $\phi_{SU(3)}$ has no contribution to the cross section and CP-odd observables for our specific process, and both the CP-odd observables ξ_{CP} and $\bar{\eta}_{CP}$ vanish when all the complex phases $\phi_{\tilde{t}}$, $\phi_{\tilde{b}}$, $\phi_{U(1)}$, and ϕ_μ are set to zero. The CP-odd observables ξ_{CP} and $\bar{\eta}_{CP}$ as the functions of $\phi_{U(1)}$ and ϕ_μ are plotted in Fig.2 and Fig.3, respectively. The curves in these two figures show that both the two observables are 2π periodic odd functions of $\phi_{U(1)}$ and ϕ_μ , i.e., they satisfy $\xi_{CP}(\pi - \phi_{U(1),\mu}) = -\xi_{CP}(\pi + \phi_{U(1),\mu})$ and $\bar{\eta}_{CP}(\pi - \phi_{U(1),\mu}) = -\bar{\eta}_{CP}(\pi + \phi_{U(1),\mu})$, when the corresponding other phases are all neglected. However, they do not have the strict symmetries for transformation $\phi_{U(1)} \rightarrow \pi - \phi_{U(1)}$ or $\phi_\mu \rightarrow \pi - \phi_\mu$. Fig.4

plots the CP-odd observables as functions of $\phi_{\tilde{t}}$, where the other phases are zero, because the strength of top-stop-gluino coupling depends on the value of $\phi_{\tilde{t}}$, and comparatively the contributions from squark mixing phases to non-QCD sectors are small such that they can be omitted in general cases. From the curve we can see that the CP violation is maximized when $\phi_{\tilde{t}} = \frac{\pi}{4}$, the absolute values of ξ_{CP} and $\bar{\eta}_{CP}$ being over one percent, which is much larger than in the usual cases.

In Fig.5(a,b,c,d) we depict the dependences of the CP-violating parameters ξ_{CP} and $\bar{\eta}_{CP}$ on the c.m. energy $\sqrt{\hat{s}}$, with the contributions from gluino, chargino, neutralino and overall diagrams, respectively. The threshold effect near the energy region $\sqrt{\hat{s}} = 2m_t$ can be seen obviously in these figures. From the figure 5(a) and 5(c) it is shown that at the position of $\sqrt{\hat{s}} \sim 2m_{\tilde{t}_2} = 800 \text{ GeV}$ there is an abrupt turning-point in ξ_{CP} and a spike in $\bar{\eta}_{CP}$ in each of the curves, which are caused by the resonance effects mainly coming from the triangle diagram including the coupling $\gamma\tilde{t}\tilde{t}$, which occurs only in gluino and neutralino sectors. Fig.5 (b) shows that the curve of $\bar{\eta}_{CP}$ contributed by chargino sector reaches its maximal and minimal values at the positions of $\sqrt{\hat{s}} \sim 2m_{\tilde{\chi}_{1,2}^+} = 400, 580 \text{ GeV}$, respectively, due to the resonance effects happening in the coupling $\gamma\tilde{\chi}^+\tilde{\chi}^-$. However, the curve of ξ_{CP} has an almost plain maximum region in the range of 400 GeV to 580 GeV. It is because of the emergence of several individual resonance effects originating from the diagrams of chargino sector at the positions of $\sqrt{\hat{s}} \sim 2m_{\tilde{b}_{1,2}}, 2m_{\tilde{\chi}_{1,2}^+}$, where $m_{\tilde{b}_{1,2}} \sim 270, 280 \text{ GeV}$, $m_{\tilde{\chi}_{1,2}^+} = 200, 290 \text{ GeV}$. That leads to the CP-violation parameter $\bar{\eta}_{CP}$ contributed from all sectors has two peaks in Fig.5(d), one is around $\sqrt{\hat{s}} \sim 800 \text{ GeV}$ and another is about $\sqrt{\hat{s}} \sim 500 \text{ GeV}$. From the magnitude order of the curves we may infer that the chargino loop diagrams impress the CP-odd observable quite considerably and in some region its CP-violating effect may be comparable to the contribution from gluino sector, whereas that from neutralino is always the smallest among the three sectors. In addition, Fig.5 also shows that the absolute values of both the two CP-odd observables approach to zero with increasing $\sqrt{\hat{s}}$, when the c.m.s. energy of photons is beyond 800 GeV.

We vary the parameter $\tan \beta$ from 0.5 to 100 with other parameters being taken as in Eq.(3.2). The results are depicted in Fig.6, among which (a) stands for the chargino sector contribution and (b) for contribution from neutralino sector. We find that the absolute values of both the two observables decrease steadily with increasing β , except at the end of each curve of Fig.6(a) where $\beta > 1.4$. And generally the contributed parts of ξ_{CP} ($\bar{\eta}_{CP}$) from the chargino and neutralino sectors

have opposite signs, so that they cancel with each other to some extent. In Fig.7 and Fig.8, the two observables as the functions of $|M_{SU(2)}|$ and $|\mu|$ are plotted, respectively. The curves in both figures have the similar property. In both the two figures it is shown that the CP violating effect is quite weak when $|M_{SU(2)}|$ or $|\mu|$ is near zero, because that in these cases the mass of the lightest chargino or neutralino is very small and thus the contributions from the CP-violating phases are suppressed. We can also see from the figure that each curve has a sharp slope at the position of $|M_{SU(2)}| \sim 260 \text{ GeV}$ (Fig.7) or $|\mu| \sim 230 \text{ GeV}$ (Fig.8) due to the resonance effects when $\sqrt{\hat{s}} = 600 \text{ GeV} \sim 2m_{\tilde{\chi}_2^+}$. And when the absolute value of $M_{SU(2)}$ or $|\mu|$ becomes larger, the CP-violating effect gets lower steadily. Fig.9 plots the CP-violating parameters as functions of $|M_{U(1)}|$, which reflects the impression of U(1) mass parameter on the CP violation through neutralino diagonalizing matrix N and its mass spectra. The curves go down steadily except that in the region of $M_{U(1)} < 60 \text{ GeV}$, ξ_{CP} rises sharply. In Fig.10 we only consider the contribution from QCD sector and plot the dependence of CP violation on the mass of gluino($m_{\tilde{g}} = |M_{SU(3)}|$). From the figure one can see the curves rise sharply with increasing gluino mass at the low $|M_{SU(3)}|$ region, then go down steadily as $|M_{SU(3)}|$ becomes larger. The maximal values are 1.15% for ξ_{CP} and 0.98% for $\bar{\eta}_{CP}$ around the position of $M_{SU(3)} \sim 200 \text{ GeV}$.

IV. Summary

In this work we have studied all the contributions to the CP-odd observables in the process $\gamma\gamma \rightarrow t\bar{t}$ in the frame of the MSSM with complex soft breaking SUSY parameters. The CP violating effects in this process are related to the complex phases of μ , A_t , A_b , $M_{SU(3)}$ and $M_{U(1)}$ through the diagonalization of the complex stop, sbottom, chargino and neutralino mass matrices. We introduce the CP-odd observables ξ_{CP} and $\bar{\eta}_{CP}$ to describe the CP violating effects in polarized and unpolarized photon collision cases, respectively. Our calculation shows that they can be different from zero and are typically of the order of $10^{-4} \sim 10^{-2}$, if CP violation really exists. The CP violating effect contributed by gluino sector is generally the most important, whereas neutralino and chargino exchanges in the loop diagrams play less important roles, but cannot be neglected in some cases. We find that it is possible to observe the CP violating effects in top quark pair production via po-

larized and unpolarized photon fusions by using optimal observables and favorable parameters. Therefore, probing CP violation in this process is a rather prospective goal for future photon-photon colliders.

Acknowledgement: These work was supported in part by the National Natural Science Foundation of China(project numbers: 19675033) and the Youth Science Foundation of the University of Science and Technology of China.

Appendix: Transformation Matrices U, V and N

One can get the physical mass spectra and transformation matrices of charged gauginos when diagonalizing the following mass matrix:

$$X = \begin{pmatrix} M_{SU(2)} & m_W \sqrt{2} \sin \beta \\ m_W \sqrt{2} \cos \beta & |\mu| e^{i\phi_\mu} \end{pmatrix}, \quad (A.1)$$

where the complex phase of $M_{SU(2)}$ has been neglected because it is a trivial one. The two 2×2 unitary matrices U, V are defined to diagonalize the matrix X , namely,

$$U^* X V^\dagger = X_D, \quad (A.2)$$

where X_D is a diagonal matrix with non-negative entries. The two diagonal elements of this matrix are worked out in general case as

$$M_\pm^2 = \frac{1}{2} \left\{ M_{SU(2)}^2 + |\mu|^2 + 2m_W^2 \pm \left[(M_{SU(2)}^2 - |\mu|^2)^2 + 4m_W^4 \cos^2 2\beta + 4m_W^2 (M_{SU(2)}^2 + |\mu|^2 + 2M_{SU(2)}|\mu| \sin 2\beta \cos \phi_\mu) \right]^{1/2} \right\}, \quad (A.3)$$

which just stand for the masses of chargino $\tilde{\chi}_1^+$ and $\tilde{\chi}_2^+$. The diagonalizing matrices U and V have very complicated forms depending on the complex phase of μ . In general, we can write

$$U = \begin{pmatrix} \cos \theta_U e^{i(\phi_1 + \xi_1)} & \sin \theta_U e^{i(\phi_1 + \xi_1 + \delta_U)} \\ -\sin \theta_U e^{i(\phi_2 + \xi_2 - \delta_U)} & \cos \theta_U e^{i(\phi_2 + \xi_2)} \end{pmatrix}$$

$$V = \begin{pmatrix} \cos \theta_V e^{i(\phi_1 - \xi_1)} & \sin \theta_V e^{i(\phi_1 - \xi_1 + \delta_V)} \\ -\sin \theta_V e^{i(\phi_2 - \xi_2 - \delta_V)} & \cos \theta_V e^{i(\phi_2 - \xi_2)} \end{pmatrix}, \quad (A.4)$$

where the ξ_1 and ξ_2 can be any arbitrarily chosen phases. It indicates the matrices U and V satisfying Eq.(A.2) are not unique, namely, some arbitrary phases may be introduced into the physical fields. But our calculation shows that they have no effects on the CP-odd observables. The explicit forms of the other constant angles and phases depending on the input parameters are given as

$$\begin{aligned}
\tan \theta_U &= \sqrt{\frac{M_+^2 - M_{SU(2)}^2 - 2m_W^2 \sin^2 \beta}{M_+^2 - |\mu|^2 - 2m_W^2 \cos^2 \beta}}, \\
\tan \theta_V &= \sqrt{\frac{M_-^2 - M_{SU(2)}^2 - 2m_W^2 \cos^2 \beta}{M_-^2 - |\mu|^2 - 2m_W^2 \sin^2 \beta}}, \\
e^{i2\phi_1} &= \frac{\cos \theta_U}{\cos \theta_V} \cdot \frac{M_+^2 + M_{SU(2)}|\mu| \tan \beta e^{i\phi_\mu} - 2m_W^2 \sin^2 \beta}{M_+ (M_{SU(2)} + |\mu| \tan \beta e^{i\phi_\mu})}, \\
e^{i2\phi_2} &= \frac{\cos \theta_V}{\cos \theta_U} \cdot \frac{M_-^2 + M_{SU(2)}|\mu| \tan \beta e^{i\phi_\mu} - 2m_W^2 \sin^2 \beta}{M_- (M_{SU(2)} \tan \beta + |\mu| e^{-i\phi_\mu})}, \\
e^{i\delta_U} &= \frac{M_{SU(2)} + |\mu| e^{i\phi_\mu} \tan \beta}{|M_{SU(2)} + |\mu| e^{i\phi_\mu} \tan \beta|}, \\
e^{i\delta_V} &= \frac{M_{SU(2)} \tan \beta + |\mu| e^{i\phi_\mu}}{|M_{SU(2)} \tan \beta + |\mu| e^{i\phi_\mu}|}, \tag{A.5}
\end{aligned}$$

where M_\pm can be evaluated from Eq.(A.3).

As for the case of neutral gauginos, we can obtain the transformation matrix N by diagonalizing the following 4×4 mass matrix:

$$Y = \begin{pmatrix} |M_{U(1)}| e^{i\phi_{U(1)}} & 0 & -m_Z \sin \theta_W \cos \beta & m_Z \sin \theta_W \sin \beta \\ 0 & M_{SU(2)} & m_Z \cos \theta_W \cos \beta & -m_Z \cos \theta_W \sin \beta \\ -m_Z \sin \theta_W \cos \beta & m_Z \cos \theta_W \cos \beta & 0 & -|\mu| e^{i\phi_\mu} \\ m_Z \sin \theta_W \sin \beta & -m_Z \cos \theta_W \sin \beta & -|\mu| e^{i\phi_\mu} & 0 \end{pmatrix}. \tag{A.6}$$

Again the parameter $M_{SU(2)}$ can be set to be real. The transformation matrix N is chosen such that

$$N^* Y N^\dagger = Y_D \tag{A.7}$$

and should be unitary. Y_D is a 4×4 diagonal matrix with four non-negative entries. To obtain the mass spectra Y_D and the transformation matrix N , we separate Y

into the real part Y_1 and the imaginary part Y_2 ($Y = Y_1 + iY_2$), and define an 8×8 matrix as

$$Y' = \begin{pmatrix} Y_1 & -Y_2 \\ -Y_2 & -Y_1 \end{pmatrix}. \quad (A.8)$$

We have proved that, if the eight eigenvalues of Y' can be worked out, the four positive ones among them will just be the four entries of Y_D , i.e., the physical masses of neutralino. Meanwhile, if the four corresponding eigenvectors of Y' to the four positive eigenvalues are denoted as $(R_{i1} \ R_{i2} \ R_{i3} \ R_{i4} \ I_{i1} \ I_{i2} \ I_{i3} \ I_{i4})^T$, where i is from 1 to 4, the transformation matrix N will take the form of

$$N = \begin{pmatrix} R_{11} - iI_{11} & R_{12} - iI_{12} & R_{13} - iI_{13} & R_{14} - iI_{14} \\ R_{21} - iI_{21} & R_{22} - iI_{22} & R_{23} - iI_{23} & R_{24} - iI_{24} \\ R_{31} - iI_{31} & R_{32} - iI_{32} & R_{33} - iI_{33} & R_{34} - iI_{34} \\ R_{41} - iI_{41} & R_{42} - iI_{42} & R_{43} - iI_{43} & R_{44} - iI_{44} \end{pmatrix}. \quad (A.9)$$

References

- [1] J. H. Christensen, J. Cronin, V. F. Fitch and R. Turlay, Phys. Rev. Lett. **13**, 138 (1964).
- [2] S. Weinberg, Phys. Rev. Lett. **63**, 2333 (1989).
- [3] M. Kobayashi and T. Maskawa, Prog. Theor. Phys. **49**, 652 (1973).
- [4] A. G. Cohen, D. B. Kaplan, and A. Nelson, Annu. Rev. Nucl. Part. Phys. **43**, 27 (1993).
- [5] A. Brandenburg, J. P. Ma, and O. Nachtmann, Z. Phys. C **55**, 115 (1992)
- [6] CDF Collaboration, F. Abe et al., Phys. Rev. Lett. **74**, 2626 (1995);
D0 Collaboration, S. Abachi et al., ibid. **74**, 2632 (1995).
- [7] A. Bartl, E. Christova, T. Gajdosik and W. Majerotto, HEPHY-PUB 672/97,
UWThPh-1997-28, hep-ph/9709219.

- [8] B. Grzadkowski and Z. Hioki, IFT-07-96, TOKUSHIMA 96-01, hep-ph/9604301; B. Grzadkowski and Z. Hioki, Phys. Lett. **B391**, 172 (1997).
- [9] P. Poulose and S. D. Rindani, Phys. Lett. **B349**, 379 (1995).
- [10] P. Poulose and S. D. Rindani, Phys. Lett. **B383**, 212 (1996); Phys. Rev. **D54**, 4326 (1996).
- [11] P. Poulose and Saurabh D. Rindani, Phys. Rev. **D57**, 5444 (1998).
- [12] C. R. Schmidt, Phys. Lett. **B293**, 111 (1992); C. R. Schmidt, M. E. Peskin, Phys. Rev. Lett. **69**, 410 (1992).
- [13] W. Bernreuther and A. Brandenburg, Phys. Rev. **D49**, 4481 (1994).
- [14] P. Haberl, O. Nachtmann and A. Wilch, Phys. Rev. **D53**, 4875 (1996).
- [15] B. Grzadkowski, B. Lampe and K. J. Abraham, Phys. Lett. **B415**, 193 (1997).
- [16] Ma Wen-Gan, Li Chong-Sheng and Han Liang, Phys. Rev. **D53**, 1304 (1996); (E:) V. Barger and R. J. N. Philips, *ibid.* **39**, 3310 (1989); A. C. Bawa et al., Z. Phys. **C47**, 75 (1990); Han Liang, Cheng-Guo Hu, Chong-Sheng Li, and Ma Wen-Gan, Phys. Rev. **D54**, 2363 (1996).
- [17] Harald Anlauf, Werner Bernreuther, and Arnd Brandenburg, Phys. Rev. **D52**, 3803 (1995).
- [18] Han Liang, Ma Wen-Gan, and Yu Zeng-Hui, Phys. Rev. **D56**, 265 (1997).
- [19] H. E. Haber, G. L. Kane, Phys. Rep. **177** (1985) 75; J. Gunion and H. E. Haber, Nucl. Phys. **B272** (1986) 1.
- [20] M. Dugan, B. Grinshtein, L. Hall, Nucl. Phys. **B255** (1985) 418; W. Bernreuther, M. Suzuki, Rev. Mod. Phys. 08 (1991) 313.
- [21] A. Denner, Fortschr. Phys. **41**, 4 (1993), p307.
- [22] J. Bjorken and S. Drell, Relativistic Quantum Mechanics (McGraw-Hill, New-York, 1964).

- [23] Gregory Mahlon and Stephen Parke, Phys. Rev. **D53**, 4886 (1996).
- [24] M. Dugan, B. Grinshtain, and L. Hall, Nucl. Phys. **B255**, 413 (1985); W. Bernreuther and M. Suzuki, Rev. Mod. Phys. **63**, 313 (1991).

Figure captions

Fig.1 The Feynman diagrams at tree level and the MSSM one-loop order diagrams contributing to the CP violation for process $\gamma\gamma \rightarrow t\bar{t}$. (a) tree level diagram; (b)-(e) vertex diagrams; (f)-(h) box diagrams; (i) quartic coupling diagram, and (j) self-energy diagrams. The \tilde{q} and \tilde{s} in Fig.1 respectively denote the following corresponding particles: In figures (b), (c), (f) and (h), $\tilde{q} = \tilde{b}_{1,2}$, $\tilde{s} = \tilde{\chi}_{1,2}^+$, whereas in diagrams (d), (e), (g), (i) and (j), there are three sets of combinations: $\tilde{q} = \tilde{t}_{1,2}$, $\tilde{s} = \tilde{g}$; $\tilde{q} = \tilde{b}_{1,2}$, $\tilde{s} = \tilde{\chi}_{1,2}^+$; and $\tilde{q} = \tilde{t}_{1,2}$, $\tilde{s} = \tilde{\chi}_{1,2,3,4}^0$. The diagrams with incoming photons exchanged are not shown in the figures except for (i).

Fig.2 The CP-violating parameters as the functions of $\phi_{U(1)}$ with $\phi_{\tilde{t},\tilde{b}} = \phi_\mu = \phi_{SU(3)} = 0$. The solid line is for ξ_{CP} and the dashed line is for $\bar{\eta}_{CP}$.

Fig.3 The CP-violating parameters as the functions of ϕ_μ with $\phi_{\tilde{t},\tilde{b}} = \phi_{U(1)} = \phi_{SU(3)} = 0$. The solid line is for ξ_{CP} and the dashed line is for $\bar{\eta}_{CP}$.

Fig.4 The CP-violating parameters as the functions of $\phi_{\tilde{t}} - \phi_{SU(3)}$ with $\phi_\mu = \phi_{U(1)} = 0$. The solid line is for ξ_{CP} and the dashed line is for $\bar{\eta}_{CP}$.

Fig.5 The CP-violating parameters as the functions of $\sqrt{\hat{s}}$ with the values of other parameters shown in Eq.(3.2). (a) the gluino sector only. (b) the chargino sector only. (c) the neutralino sector only. (d) all three sectors together. The solid line is for ξ_{CP} and the dashed line is for $\bar{\eta}_{CP}$.

Fig.6 The CP-violating parameters as the functions of β with the values of other parameters shown in Eq.(3.2). (a) the chargino sector only. (b) the neutralino sector only. The solid line is for ξ_{CP} and the dashed line is for $\bar{\eta}_{CP}$.

Fig.7 The CP-violating parameters contributed by chargino and neutralino sectors as the functions of $M_{SU(2)}$ with $\phi_{\tilde{t}} = \frac{\pi}{5}$ and the values of other parameters shown in Eq.(3.2). The solid line is for ξ_{CP} and the dashed line is for $\bar{\eta}_{CP}$.

Fig.8 The CP-violating parameters contributed by chargino and neutralino sectors as the functions of $|\mu|$ with $\phi_{\tilde{t}} = \frac{\pi}{5}$ and the values of other parameters shown in Eq.(3.2). The solid line is for ξ_{CP} and the dashed line is for $\bar{\eta}_{CP}$.

Fig.9 The CP-violating parameters as the functions of $M_{U(1)}$, only the neutralino sector being taken into consideration. The values of other parameters are taken as shown in Eq.(3.2). The solid line is for ξ_{CP} and the dashed line is for $\bar{\eta}_{CP}$.

Fig.10 The CP-violating parameters as the functions of $M_{SU(3)}$ by taking $\phi_{\mu} = \phi_{U(1)} = 0$. The values of other parameters are taken as shown in Eq.(3.2). The solid line is for ξ_{CP} and the dashed line is for $\bar{\eta}_{CP}$.

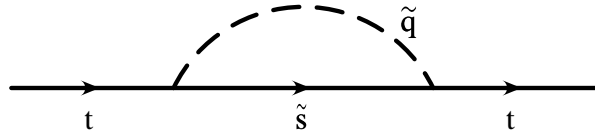
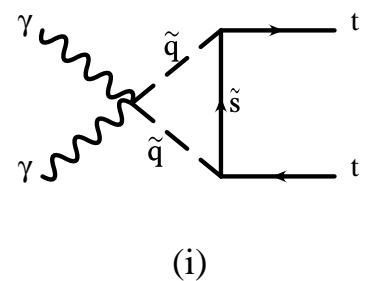
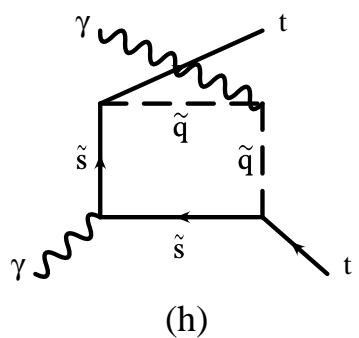
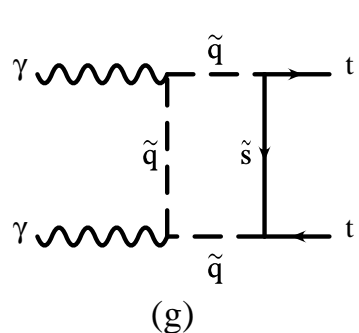
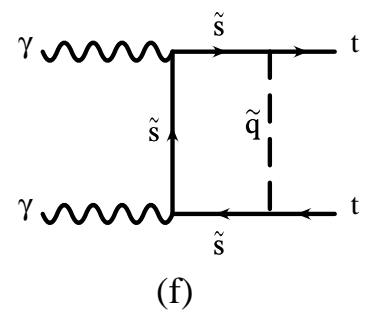
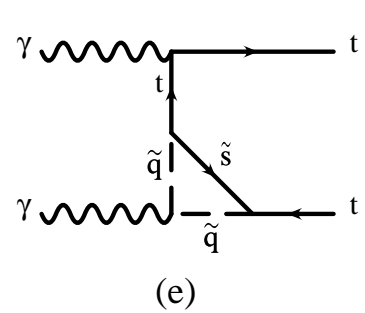
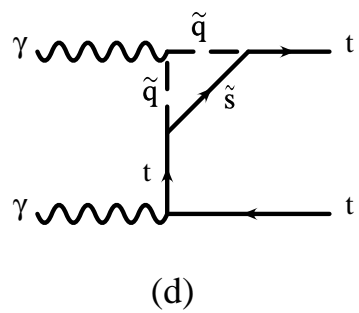
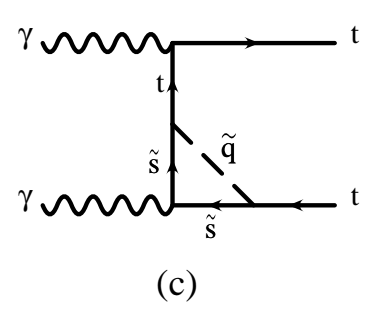
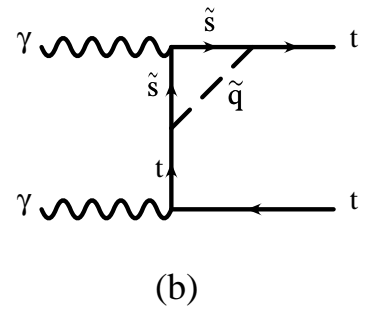
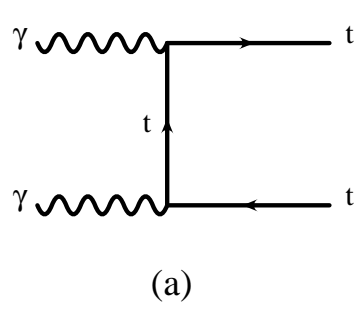


Fig.2

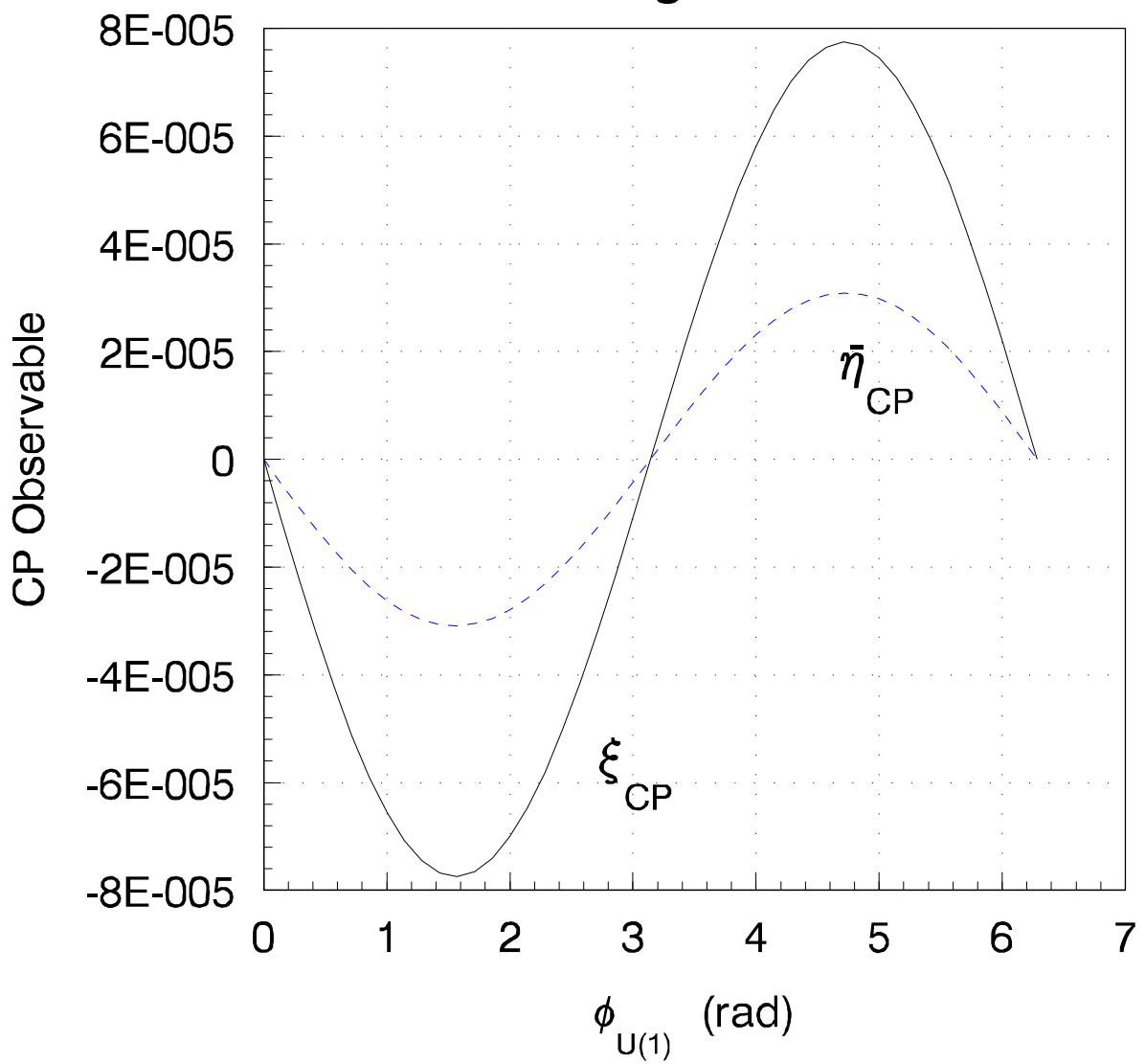


Fig.3

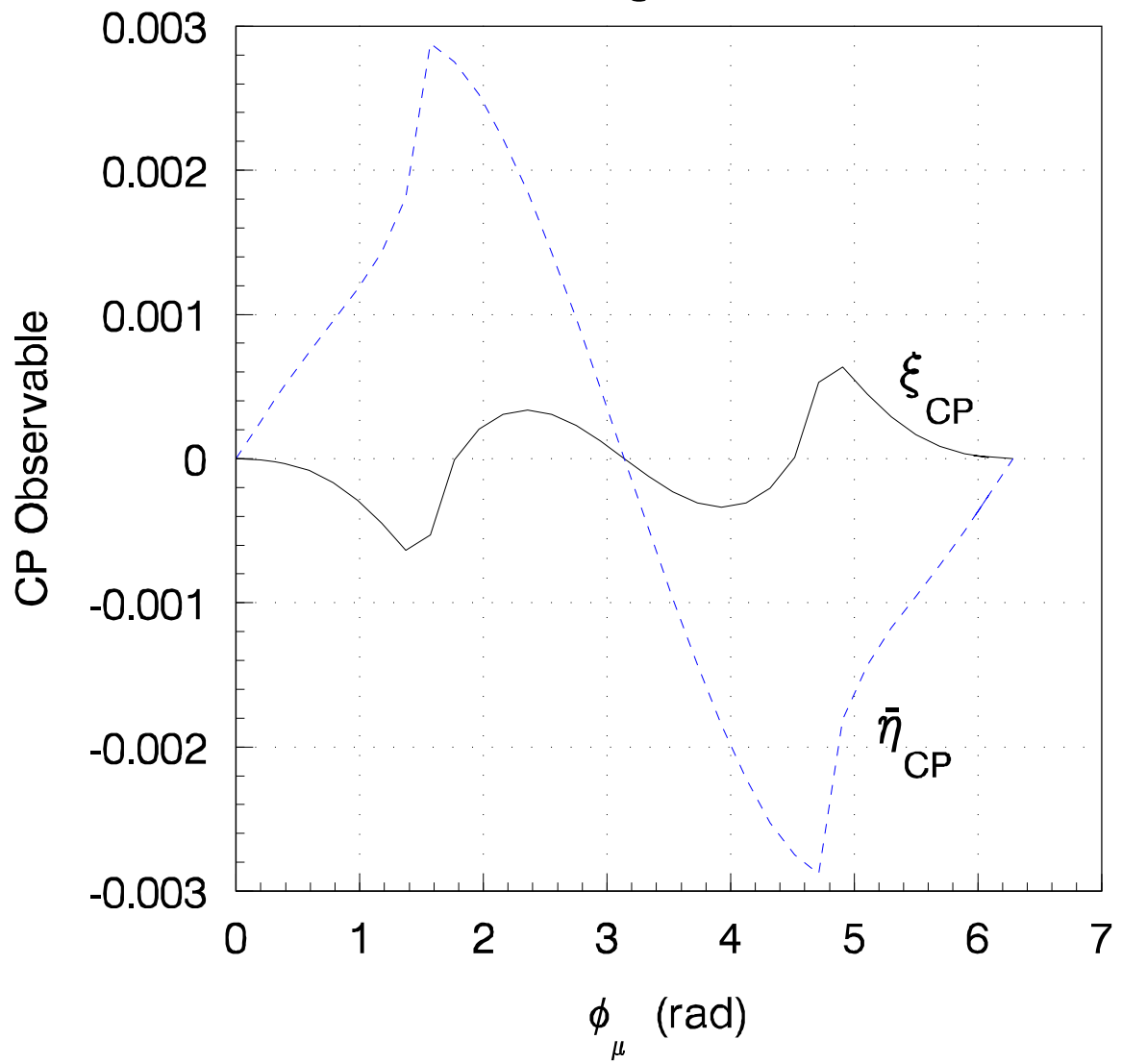


Fig.4

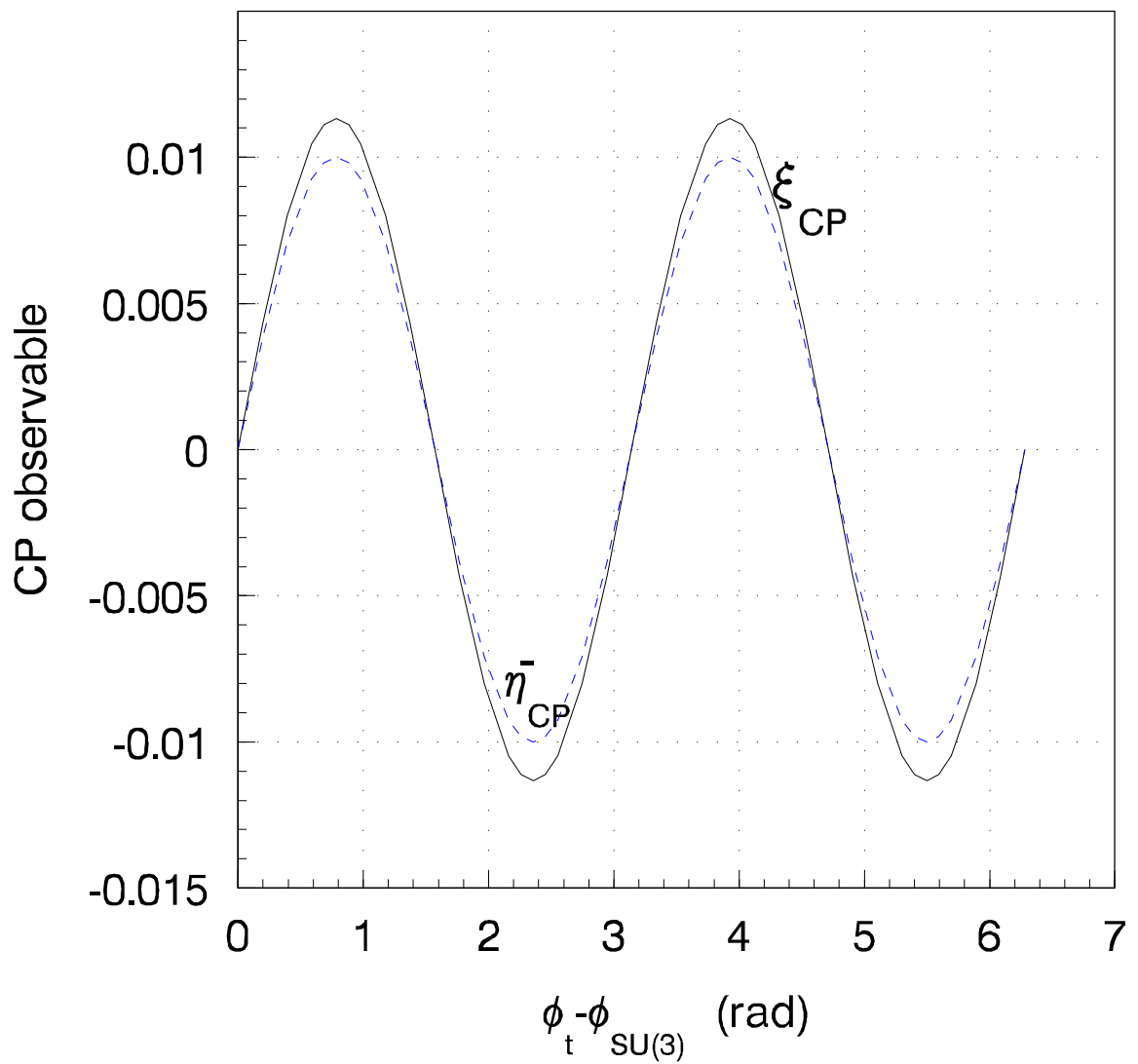


Fig.5 (a)

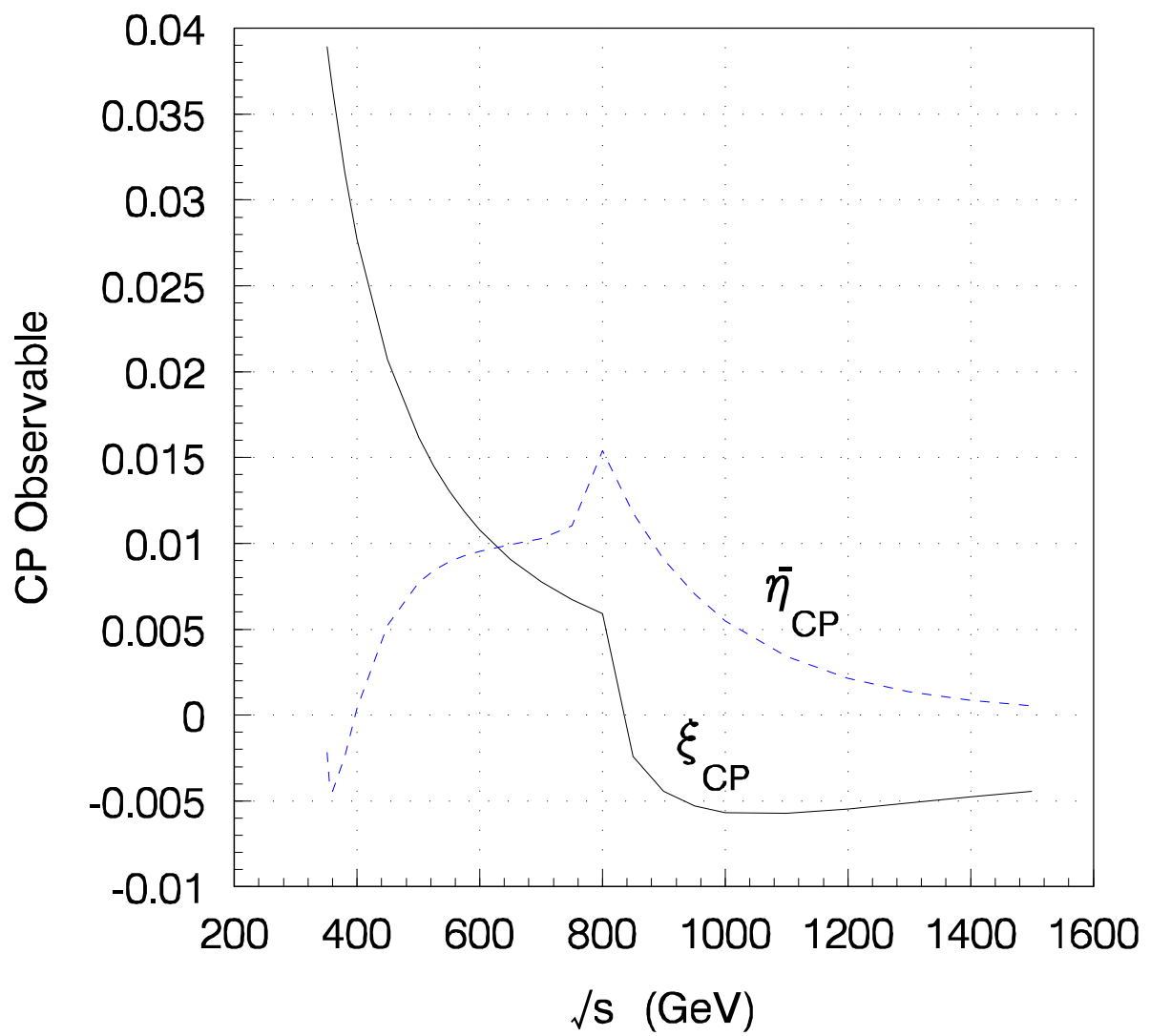


Fig.5 (b)

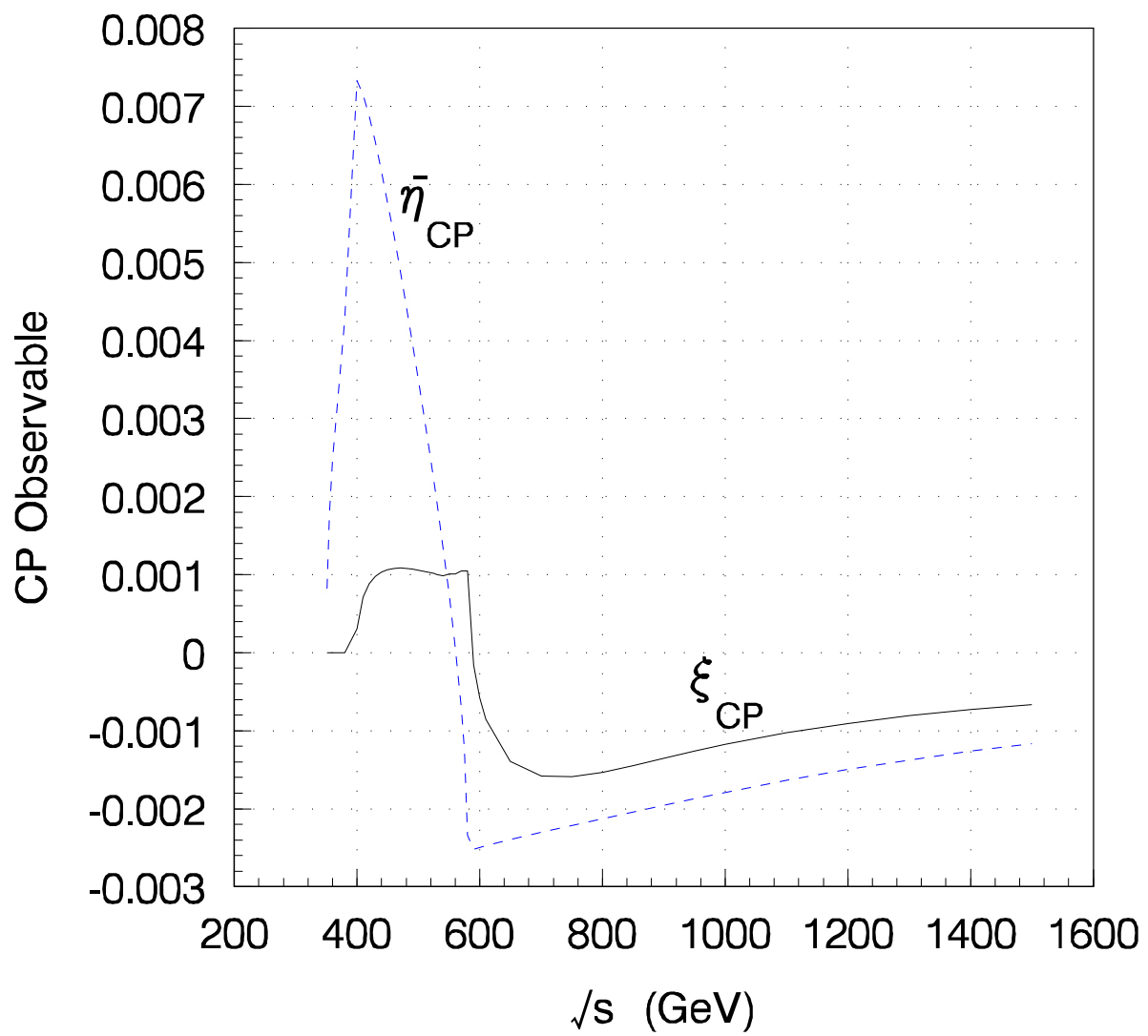


Fig.5 (c)

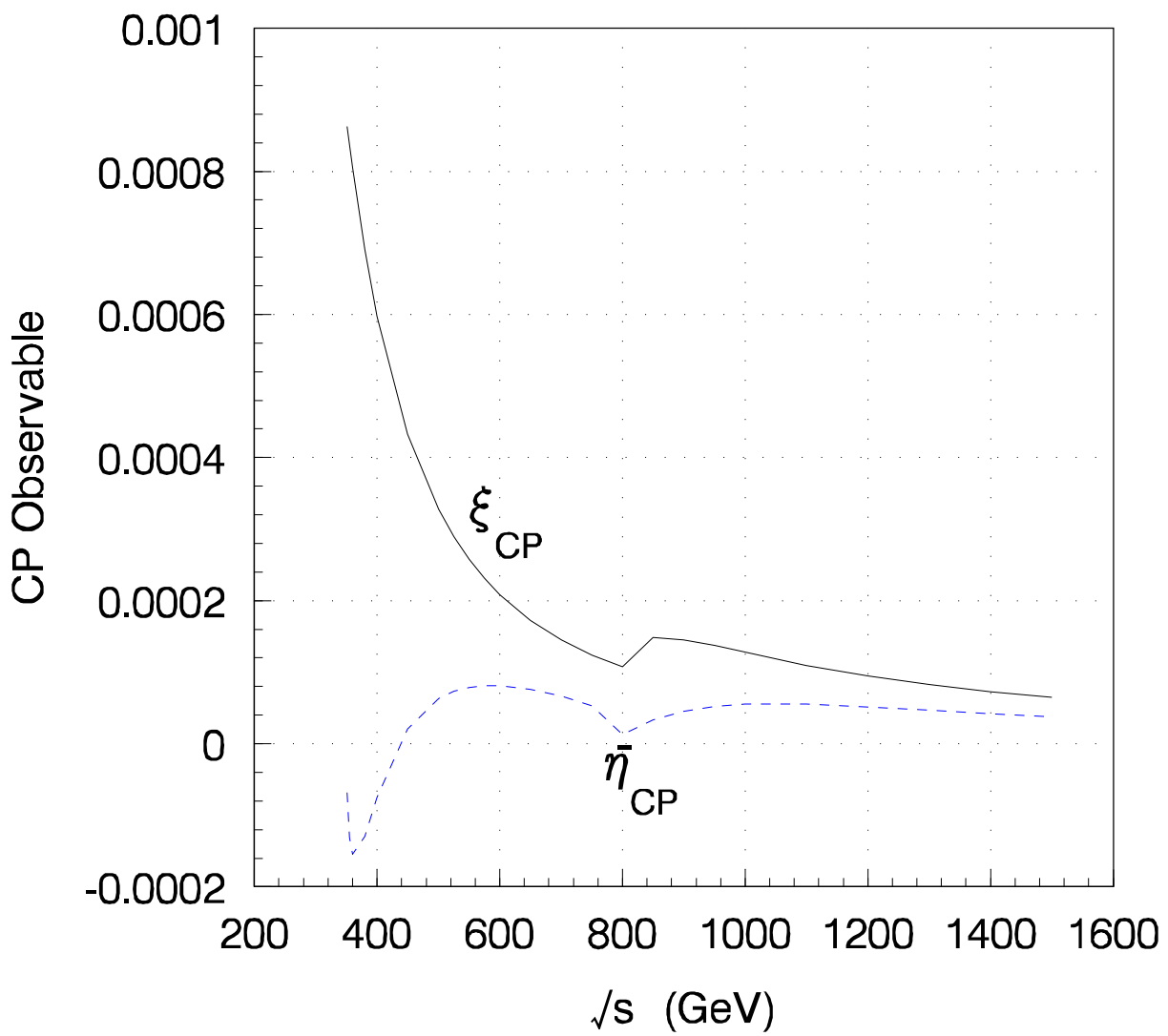


Fig.5 (d)

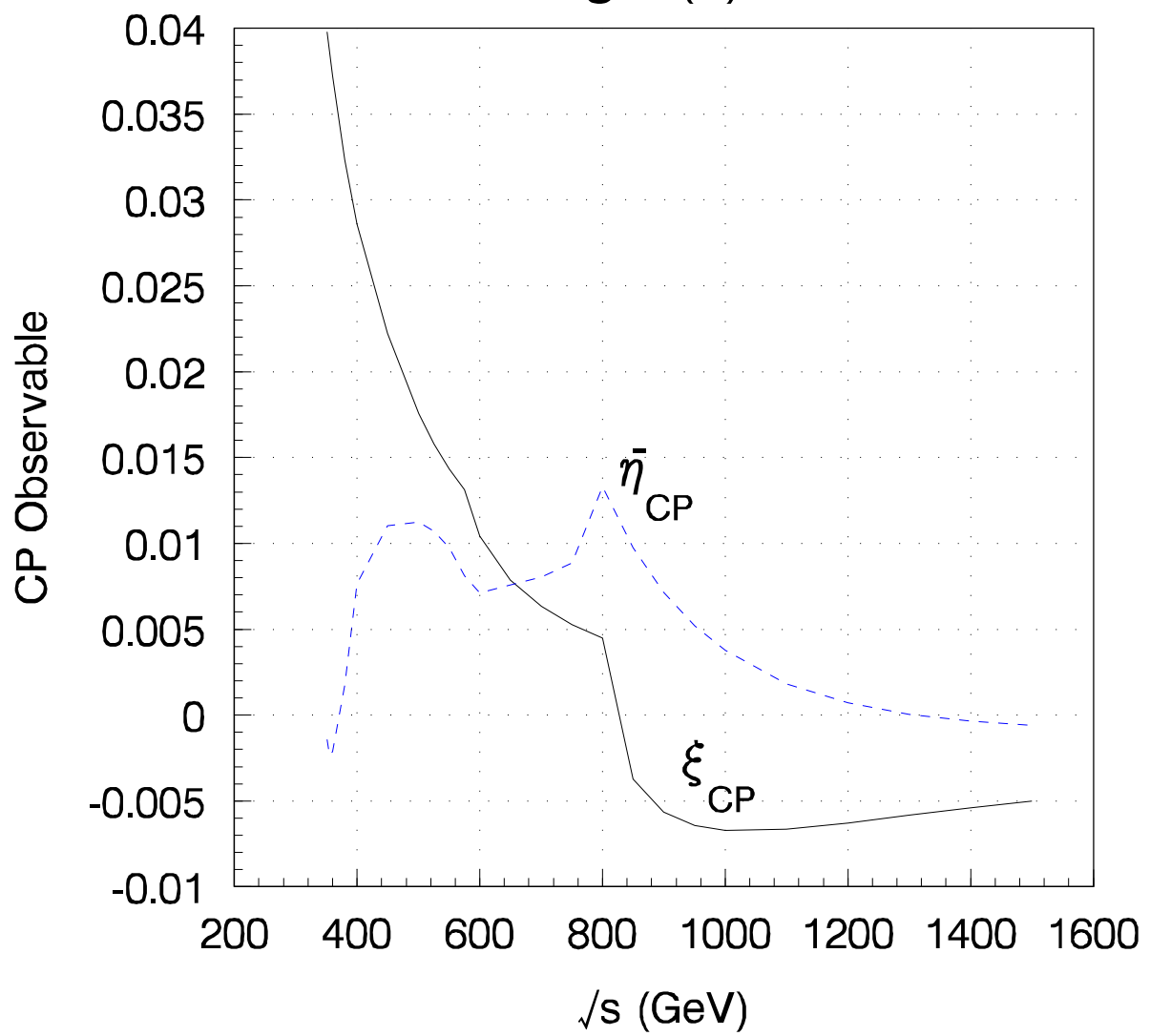


Fig.6 (a)

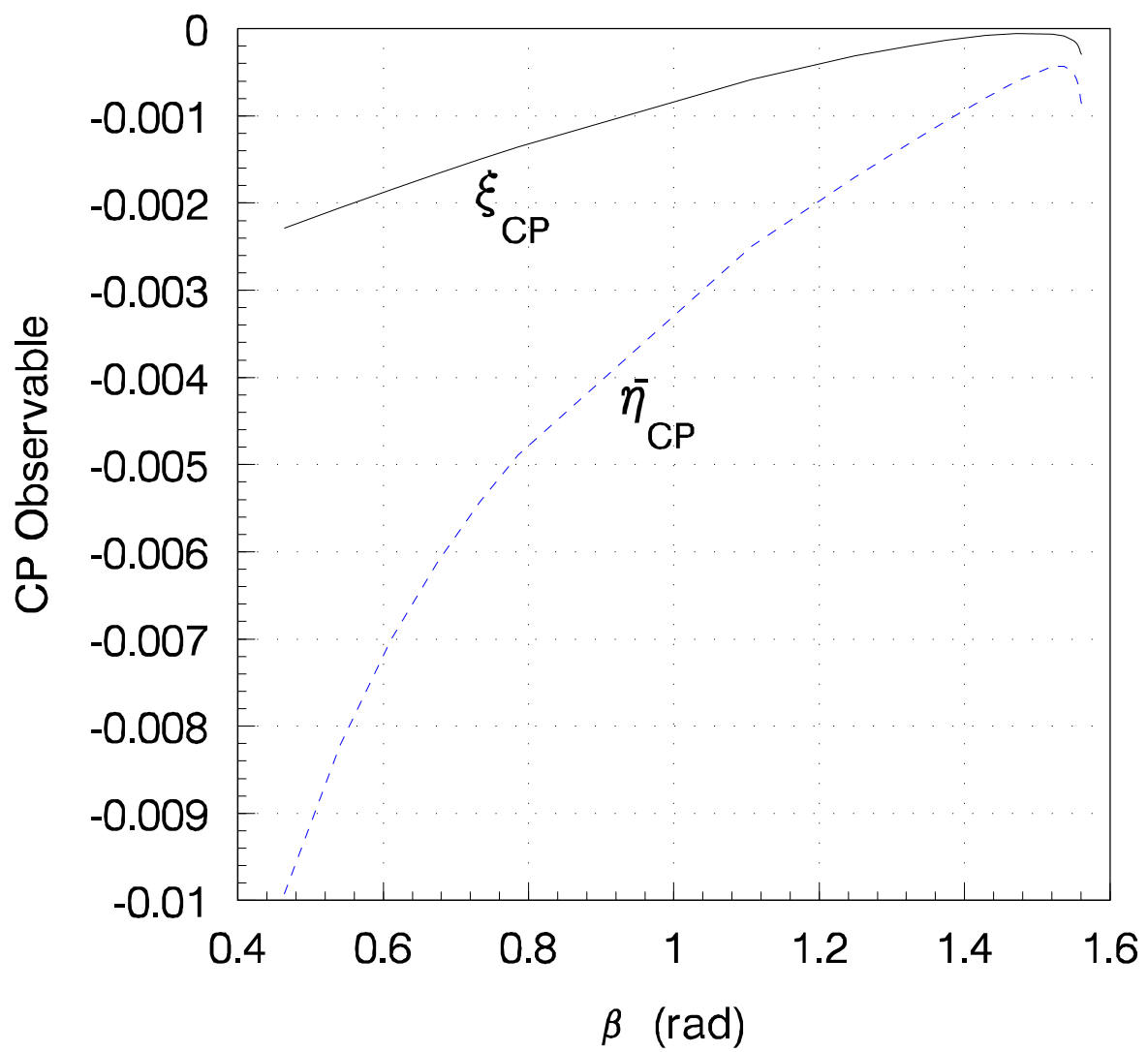


Fig.6 (b)

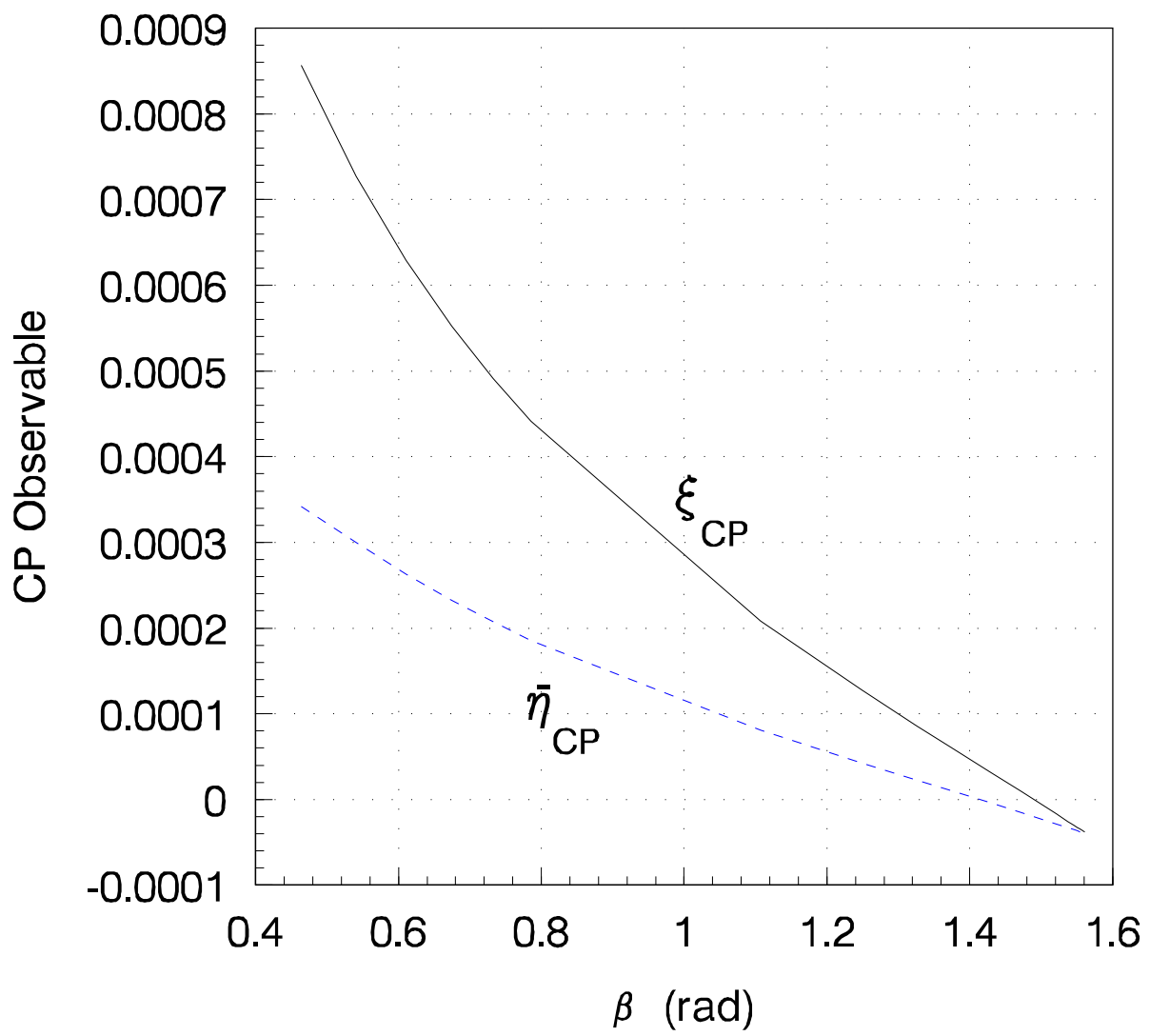


Fig.7

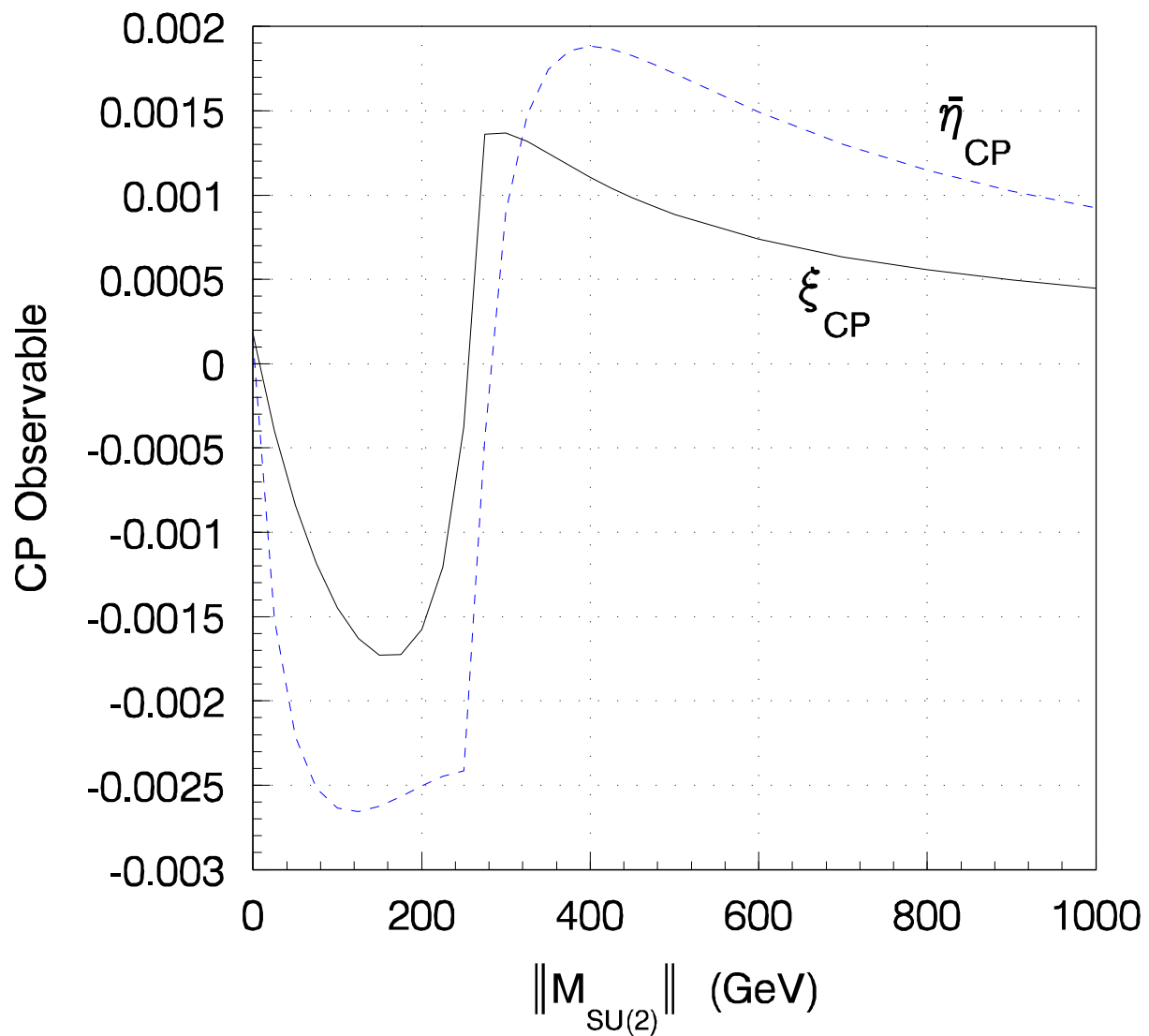


Fig.8

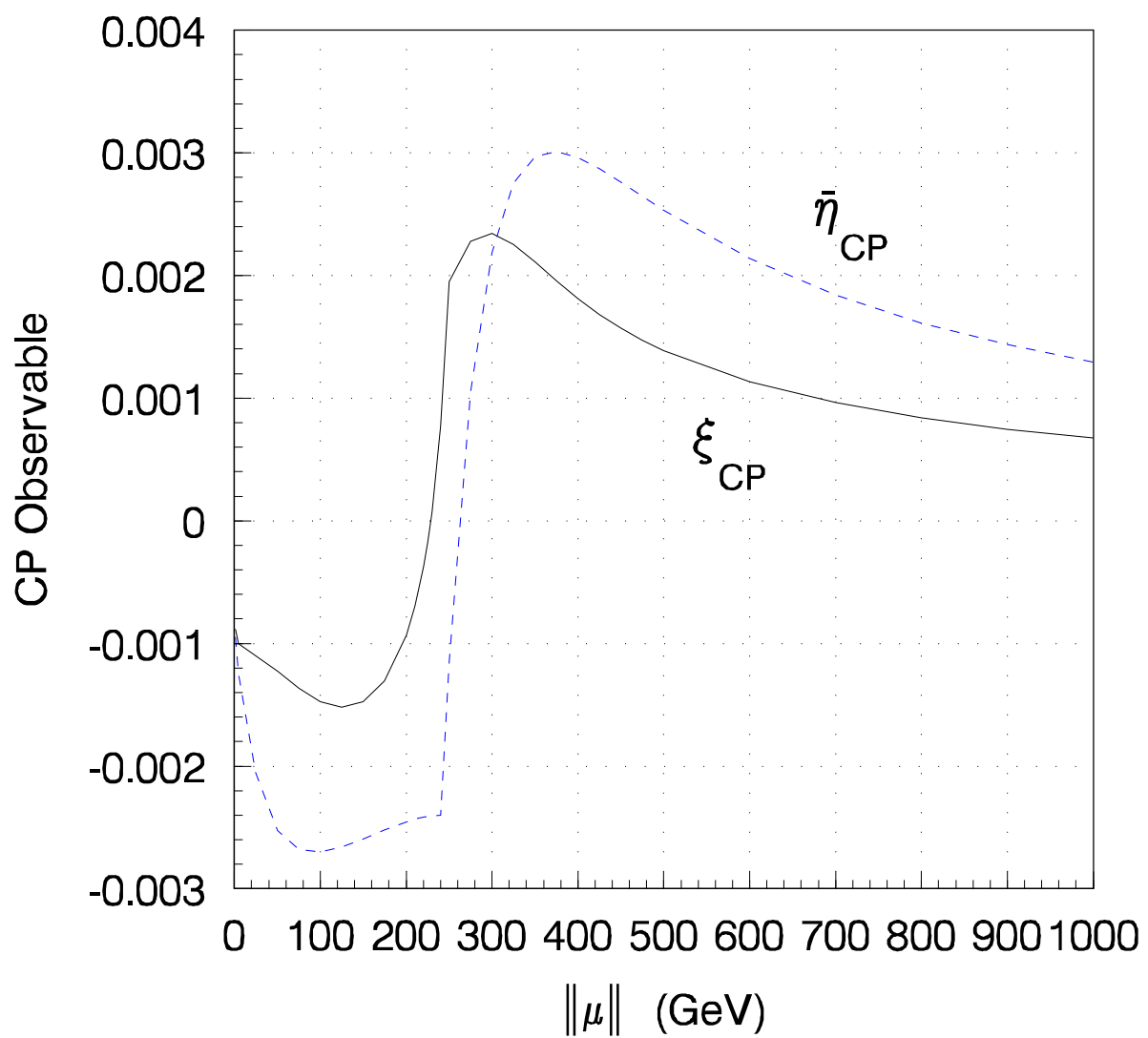


Fig.9

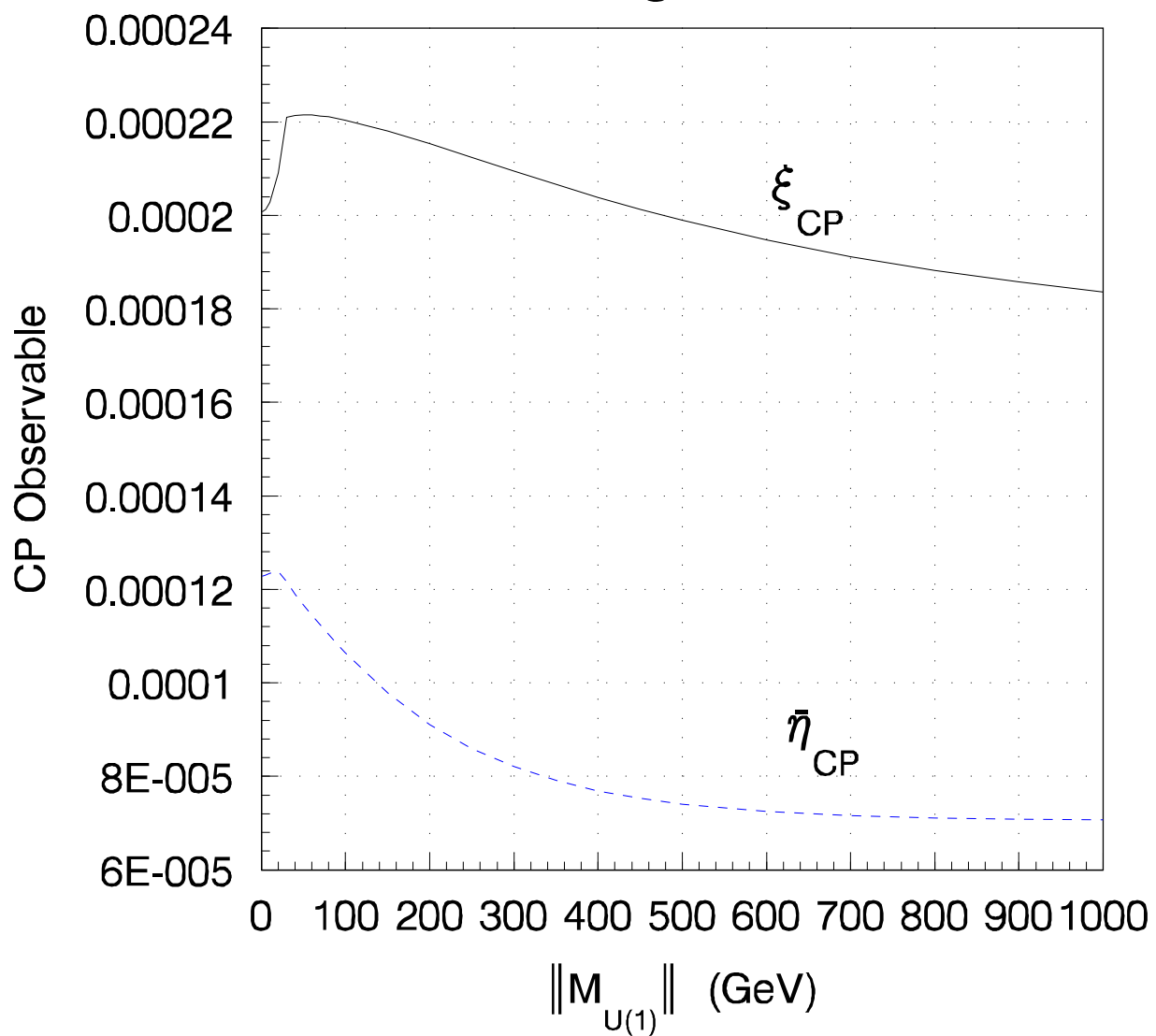


Fig.10

